The Astrophysical Journal, 806:252 (8pp), 2015 June 20 doi:10.1088/0004-637X/806/2/252

SIMULATIONS OF THE SPATIAL AND TEMPORAL INVARIANCE IN THE SPECTRA OF GRADUAL SOLAR ENERGETIC PARTICLE EVENTS

Yang Wang and Gang Qin
State Key Laboratory of Space Weather, Center for Space Science and Applied Research, Chinese Academy of Sciences, Beijing 100190, China; ywang@spaceweather.ac.cn, gqin@spaceweather.ac.cn
Received 2015 January 12; accepted 2015 May 3; published 2015 June 22

ABSTRACT

The spatial and temporal invariance in the spectra of energetic particles in gradual solar events is reproduced in simulations. Based on a numerical solution of the focused transport equation, we obtain the intensity time profiles of solar energetic particles (SEPs) accelerated by an interplanetary shock in three-dimensional interplanetary space. The shock is treated as a moving source of energetic particles with a distribution function. The time profiles of particle fluxes with different energies are calculated in the ecliptic at 1 AU. According to our model, we find that shock acceleration strength, parallel diffusion, and adiabatic cooling are the main factors in forming the spatial invariance in SEP spectra, and perpendicular diffusion is a secondary factor. In addition, the temporal invariance in SEP spectra is mainly due to the effects of adiabatic cooling. Furthermore, a spectra invariant region, which agrees with observations but is different from the one suggested by Reames et al. is proposed based on our simulations.

Key words: Sun: activity – Sun: coronal mass ejections (CMEs) – Sun: particle emission

1. INTRODUCTION

Solar energetic particle (SEP) events can roughly be divided into two categories: impulsive events and gradual events (Reames 1995, 1999). The impulsive events, characterized by low intensity and short duration, are produced by solar flares. Gradual events, usually lasting longer and having a high intensity, are related to the shocks driven by interplanetary coronal mass ejections (ICMEs). Lario et al. (2006) investigated the radial and longitudinal dependence of 4–13 MeV and 27–37 MeV proton peak intensities and fluences measured within 1 AU. They found that the peak intensities and fluences of SEP events can be approximated by $j = j_0 r^{-\alpha} \exp\left[-k\left(\phi - \phi_0\right)^2\right]$, where j is either the peak intensity or the fluence, r is the radial distance of the spacecraft, ϕ is the longitudinal angular distance between the footpoint of the observer's field line and the region of the SEP source, and ϕ_0 is the centroid of the distributions. Furthermore, the radial dependence of peak intensities and fluences of SEP events have been simulated with a focused-diffusion transport equation (Lario et al. 2007).

Generally, there are two major approaches to modeling SEP acceleration by CME driven shocks: some authors (Heras et al. 1992, 1995; Kallenrode & Wibberenz 1997; Lario et al. 1998; Kallenrode 2001; Ng et al. 2003; Wang et al. 2012; Qin et al. 2013) have adopted a "black box" model to treat the shock as a moving source in which SEPs are injected at the shock with an assumed injection strength, while a few other studies include the acceleration of SEPs by shocks (Lee 1983; Gordon et al. 1999; Zank et al. 2000; Li et al. 2003, 2005; Rice et al. 2003; Sokolov et al. 2004; Kóta et al. 2005; Tylka & Lee 2006; Zuo et al. 2011, 2013). These models have involved three important effects of acceleration and propagation mechanisms. The first effect is the acceleration process by the CME-driven shock. Zank et al. (2000) modeled the evolution of a CME-driven shock based on an "onion shell" model and this model has been further developed in a number of papers (Li et al. 2003, 2005; Rice et al. 2003). They used a magnetohydrodynamics (MHD) code to describe the evolution of the CME-driven shock in the interplanetary space, wave excitation by streaming energetic particles produced at shock. Based on the model, the simulation results can successfully explain the SEP fluxes and spectra in some multi-spacecraft observed events (Verkhoglyadova et al. 2009, 2010). The second effect is energetic particles interacting with the Alfvén waves self-consistently. Ng et al. (2003, 2012) presented a model of particle transport including streaming proton-generated Alfvén waves, in which the amplification of the Alfvén waves is determined by the anisotropy of particles. The particle diffusion coefficients can be calculated from wave intensity and wave growth rates. Their simulation results show a good agreement with the observed spectral slope and abundance ratios of heavy ions. The third effect is the realistic geometry of CME and its shock (Sokolov et al. 2004; Kóta et al. 2005). Sokolov et al. (2004) modeled particle acceleration and transport as a CME-driven shock wave propagating from 4 to 30 solar radii from the Sun. The realistic structures of CME and its shock are derived from a numerical solution of a fully three-dimensional MHD model. Their simulation results demonstrate that the diffusive shock acceleration theory can account for the increase of hundreds of MeV protons during the early stages of CME-driven shock.

SEP events measured by different spacecraft help us to understand the processes of particle acceleration and transport in the heliosphere. In some gradual events, the SEP fluxes measured by widely separated spacecraft present similar intensities within a small ~2–3 factor in different latitudes, longitudes, or radii (Reames et al. 1997; Reames 2010, 2013; Maclennan et al. 2001; McKibben et al. 2001b; Lario et al. 2003; Tan et al. 2009). This phenomenon was first proposed by McKibben (1972), and was named "reservoir" by Roelof et al. (1992). In order to interpret the reservoir phenomenon, McKibben (1972) and McKibben et al. (2001b) utilized an effective perpendicular diffusion to reduce the spatial gradients of flux, while Roelof et al. (1992) suggested a diffusion barrier produced by ICMEs or shocks. The magnitude of magnetic field increases at the outer boundary of reservoirs so that SEPs can be contained in the reservoirs for a long time. Furthermore, because the interplanetary magnetic field (IMF) has been disturbed by ICMEs, SEPs could be redistributed. Reames et al. (1996) shows that in some gradual SEP events, the spectra are invariant both in space and time. This discovery extended the original work of McKibben (1972). In Reames et al. (1996), they considered an expanding magnetic bottle of quasi-trapped particles between an ICME-driven shock and the Sun. As the magnetic bottle expanded, the SEP fluxes gradually decreased as a result of parallel diffusion and adiabatic cooling. In this sense, the magnetic bottle plays a pivotal role in the decay phase of SEP events.

In principle, the disturbances in the magnetic field caused by ICMEs can help the particles redistribute in space. However, the reservoir phenomenon cannot be simply explained as a result of the disturbances of IMF caused by ICMEs. First, in the redistribution process in Reames et al. (1996) and Reames (2013), no explicit transport mechanism can reduce the latitudinal, longitudinal, and radial gradients of SEP fluxes besides perpendicular diffusion. Second, in some SEP events, ICMEs are not directly observed by the spacecraft; the reservoir phenomenon is also observed (McKibben et al. 2001a). Third, in Reames (1999), when the observer is located at the eastern region of the shock, the onset time of temporal invariance in the SEP spectra is earlier than the shock arrival time. These results are not consistent with that of an expanding magnetic bottle.

The effect of perpendicular diffusion is important in the SEP fluxes, especially when the observer is disconnected from the shock by IMF. During the time period 1979 March 1–March 11, a gradual SEP event was detected by *Helios 1*, *Helios 2*, and *IMP 8*. The three spacecraft are located in the ecliptic near 1 AU, but at different longitudes. In the decay phase of this SEP event, the reservoir phenomenon appeared (Reames et al. 1997; Reames 1999, 2010, 2013). In this event, the in situ observation shows that an ICME was detected by *Helios* 1, but not by *Helios* 2 and *IMP* 8. The interplanetary shock was only observed by *Helios 1* and *Helios* 2, but not by *IMP* 8 (Lario et al. 2006; Reames 2010). According to the location of the three spacecraft, if the ICME was located behind the center of the shock front, then *Helios 1* was located near the center of the shock, and *Helios 2* and *IMP 8* were located at the west flank of the shock. However, the onset time of the SEP fluxes observed by the three spacecraft was very close. How could SEPs be detected by *IMP 8* before it was connected to the shock by IMF? One possible answer is the effect of perpendicular diffusion, which also possibly works in forming the reservoir phenomenon.

However, perpendicular diffusion has been a difficult problem for several decades. Observation results show various levels of perpendicular diffusion coefficients for different SEP events. For example, "dropout" phenomenon in the impulsive SEP event (Mazur et al. 2000) usually show reduced perpendicular diffusion; in order to reproduce the "dropout" phenomenon in simulations, the perpendicular diffusion coefficient $\kappa_\perp$ should be several orders of magnitude smaller than the parallel one $\kappa_\parallel$ (Giacalone et al. 2000; Dröge et al. 2010; Guo & Giacalone 2014; Wang et al. 2014). On the other hand, for some events, observation results show that the perpendicular diffusion coefficients could be comparable to the parallel ones (Dwyer et al. 1997; Zhang et al. 2003; Dresing et al. 2012). Many theories have been proposed to understand diffusion. By assuming that energetic particles' perpendicular and parallel diffusions do not interact, Jokipii (1966) developed the quasi-linear theory (QLT). According to QLT, the perpendicular diffusion coefficient is usually much smaller than the parallel one. However, it is found that interaction between parallel and perpendicular diffusion is important in theory (Kóta & Jokipii 2000) and in simulations (Qin et al. 2002a, 2002b), so the non-linear guiding center (NLGC) theory (Matthaeus et al. 2003) has been developed to describe perpendicular diffusion with the influence of parallel diffusion, which agrees with simulations much better than QLT. In addition, simulations show different levels of perpendicular diffusion, e.g., in Qin & Shalchi (2012), the magnitude of $\kappa_\perp/\kappa_\parallel$ could be as large as 10^{-1} in some conditions, and as small as 10^{-4} in other conditions.

Recently, Qin et al. (2013) proposed that the shock acceleration strength makes important contributions to the reservoir phenomenon, particularly in low-energy SEPs. In their simulations, the reservoir phenomenon is reproduced under a variety of conditions of shock acceleration strength and perpendicular diffusion. In this paper, as a continuation of Qin et al. (2013), we study the properties of SEP spectra in the decay phase. We compute the time profiles of SEP fluxes that are accelerated by interplanetary shock. In Section 2 we describe the SEP transport model and the shock model. In Section 3 we show the simulation results. In Section 4 we summarize our results.

2. MODEL

In this work, we model the transport of SEPs following previous research (e.g., Qin et al. 2006, 2013; Zhang et al. 2009; Dröge et al. 2010; He et al. 2011; Zuo et al. 2011, 2013; Wang et al. 2012, 2014). A three-dimensional focused transport equation is written as (Skilling 1971; Schlickeiser 2002; Qin et al. 2006; Zhang et al. 2009)

$$\frac{\partial f}{\partial t} = \nabla \cdot (\boldsymbol{\kappa}_\perp \cdot \nabla f) - \left(v\mu\hat{\boldsymbol{b}} + \boldsymbol{V}^{\mathrm{sw}}\right) \cdot \nabla f + \frac{\partial}{\partial \mu}\left(D_{\mu\mu}\frac{\partial f}{\partial \mu}\right) + p\left[\frac{1-\mu^2}{2}\left(\nabla \cdot \boldsymbol{V}^{\mathrm{sw}} - \hat{\boldsymbol{b}}\hat{\boldsymbol{b}} : \nabla \boldsymbol{V}^{\mathrm{sw}}\right) + \mu^2\hat{\boldsymbol{b}}\hat{\boldsymbol{b}} : \nabla \boldsymbol{V}^{\mathrm{sw}}\right]\frac{\partial f}{\partial p} - \frac{1-\mu^2}{2}\left[-\frac{v}{L} + \mu\left(\nabla \cdot \boldsymbol{V}^{\mathrm{sw}} - 3\hat{\boldsymbol{b}}\hat{\boldsymbol{b}} : \nabla \boldsymbol{V}^{\mathrm{sw}}\right)\right]\frac{\partial f}{\partial \mu}, \tag{1}$$

where $f(\boldsymbol{x}, \mu, p, t)$ is the gyrophase-averaged distribution function; $\boldsymbol{x}$ is the position in a non-rotating heliographic coordinate system; t is the time; μ, p, and v are the particle pitch-angle cosine, momentum, and speed, respectively, in the solar wind frame; $\hat{\boldsymbol{b}}$ is a unit vector along the local magnetic field; $\boldsymbol{V}^{\mathrm{sw}} = V^{\mathrm{sw}}\hat{\boldsymbol{r}}$ is the solar wind velocity; and L is the magnetic focusing length given by $L = \left(\hat{\boldsymbol{b}} \cdot \nabla \ln B_0\right)^{-1}$, with B_0 being the magnitude of the background magnetic field. The IMF is set as the Parker field model, and the solar wind speed is $400\ \mathrm{km\ s^{-1}}$. This equation includes many important particle transport effects such as particle streaming along the field line, adiabatic cooling in the expanding solar wind, magnetic focusing in the diverging IMF, and the diffusion coefficients parallel and perpendicular to the IMF.

The pitch angle diffusion coefficient model is set as (Beeck & Wibberenz 1986; Qin et al. 2005)

$$D_{\mu\mu} = D_0 \upsilon p^{q-2} \left\{ |\mu|^{q-1} + h \right\} \left(1 - \mu^2\right), \tag{2}$$

where the constant D_0 controls the magnetic field fluctuation level. The constant q is chosen as 5/3 for a Kolmogorov spectrum type of the power spectra density of magnetic field turbulence in the inertial range. Furthermore, $h = 0.01$ is chosen for the non-linear effect of pitch-angle diffusion at $\mu = 0$ in the solar wind (Qin & Shalchi 2009, 2014).

The parallel mean free path (MFP) $\lambda_\parallel$ can be written as (Jokipii 1966; Hasselmann & Wibberenz 1968; Earl 1974)

$$\lambda_\parallel = \frac{3\upsilon}{8} \int_{-1}^{+1} \frac{\left(1 - \mu^2\right)^2}{D_{\mu\mu}} d\mu, \tag{3}$$

and the parallel diffusion coefficient $\kappa_\parallel$ can be written as $\kappa_\parallel = v\lambda_\parallel/3$.

The relation between the particle momentum and the perpendicular diffusion coefficient is set as (Potgieter & Moraal 1985; Zhang 1999)

$$\boldsymbol{\kappa}_\perp = \kappa_0 \left(\frac{v}{c}\right) \left(\frac{p}{1\mathrm{GeV}c^{-1}}\right)^\alpha \left(\frac{B_e}{B}\right) \left(\boldsymbol{I} - \hat{\boldsymbol{b}}\hat{\boldsymbol{b}}\right), \tag{4}$$

where B_e is the IMF strength near the Earth, B is the magnetic field strength at the location of particle, p is particle momentum, and α is set to 1/3. Different perpendicular diffusion coefficients can be obtained by altering κ_0. Note that we use this ad hoc model for simplicity; the parameters, e.g., α could be set as other values (Zhang 1999). However, the variation of these parameters would not qualitatively change the results in this paper. There are some more complete models that have been developed to describe the particle diffusion in magnetic turbulence, such as the nonlinear guiding center theory (Matthaeus et al. 2003; Shalchi et al. 2004, 2010; Qin & Zhang 2014).

We use a time-backward Markov stochastic process method to solve the transport Equation (1). The details of this method can be found in Zhang (1999) and Qin et al. (2006). The particle injection on the shock is specified by boundary values. The chosen boundary condition follows the form (Kallenrode & Wibberenz 1997; Kallenrode 2001; Wang et al. 2012; Qin et al. 2013)

$$\begin{aligned} f_b(r, \theta, \varphi, p, t) &= a \cdot \delta(r - \upsilon_s t) \cdot S(r, \theta, \varphi, p) \\ &\quad \cdot p^{-\gamma} \cdot \xi(\theta, \varphi) \\ S(r, \theta, \varphi, p) &= \left(\frac{r}{r_c}\right)^{-\alpha(p)} \cdot \exp\left[-\frac{|\phi(\theta, \varphi)|}{\phi_c(p)}\right] \\ \xi(\theta, \varphi) &= \begin{cases} 1 & \text{if} \quad |\phi(\theta, \varphi)| \leqslant \phi_s \\ 0 & \text{otherwise,} \end{cases} \end{aligned} \tag{5}$$

where the particle are injected at $r = \upsilon_s t$, υ_s is shock speed. $\upsilon_s t = r_0 + n \cdot \Delta r$, with $n = 0, 1, 2 \cdots n_0$. Δr is the space interval between two "fresh" injections, $r_0 = 0.05$ AU is the inner boundary. r_c is set to 0.05. r is the distance between Sun and shock. ϕ is the angle between the center of shock and the point at the shock front where the particles are injected. The shock acceleration strength is set as S for specifying the particle ejection. It changes with a power law in radial distance and exponential decay toward the flank of the shock. ξ determines the spatial scale of the shock front. ϕ_s is the half width of the shock.

Table 1
Model Parameters Used in the Calculations

Parameter	Physical Meaning	Value
$V^{\rm sw}$	solar wind speed	400 km s^{-1}
v_s	shock speed	870 km s^{-1}
ϕ_s	shock width	60°
α	shock strength parameter	2[a]
ϕ_c	shock strength parameter	15°[b]
γ	injection spectrum	5.5
B_e	IMF strength near the Earth	5 nT
$\lambda_\parallel$	particle parallel radial mean free path	0.2 AU[c]
$\boldsymbol{\kappa}_\perp$	perpendicular diffusion coeffient	$0.1 \times \kappa_\parallel$[d]
r_{b0}	inner boundary	0.05 AU
r_{b1}	outer boundary	50 AU

Note.
[a] for 5 MeV protons.
[b] for 5 MeV protons.
[c] for 5 MeV protons in the ecliptic at 1 AU.
[d] for 5 MeV protons in the ecliptic at 1 AU.

3. RESULTS

The parameters used are listed in Table 1 unless otherwise stated. Note that the IMF is set as a Parker spiral, and the disturbances of IMF behind the shock are ignored. The particle energy channels are chosen as 5, 10, 20, 40, and 80 MeV. The parallel MFP depends on the momentum $\lambda_\parallel \sim p^{1/3}$. According to Qin et al. (2013), the $\kappa_\perp/\kappa_\parallel$ is set as 0.1 in the ecliptic at 1 AU. Because the shock acceleration efficient decreases as the particle energy increases, the acceleration strength parameters also change with the momentum: $\alpha \sim p^{0.3}$, $\phi_c \sim p^{-0.3}$. The observers are located in the ecliptic at 1 AU.

3.1. Temporal Invariance in the Spectra

In Figures 1 and 2, we plot the fluxes of different energy channels in cases with and without adiabatic cooling. In order to check the temporal properties of SEP spectra in the decay phase, we normalize different energy fluxes so that the fluxes have similar values soon after all of them have reached peaks. The panels show the normalized fluxes observed in the ecliptic at 1 AU, but at different longitudes E60, E20, W20, and W60. The notations E60, E20, W20, W60 are short for east 60°, east 20°, west 20°, and west 60°, respectively. East/west means the location of the observer is east/west relative to the center of the shock. The vertical lines indicate the shock's passage from the observers.

In Figure 1, the adiabatic cooling effect is included in the SEP propagation process. In the decay phase of SEP events, shock acceleration strength, adiabatic cooling, parallel diffusion, and perpendicular diffusion are the major factors that influence the flux behavior. In the four panels, at all

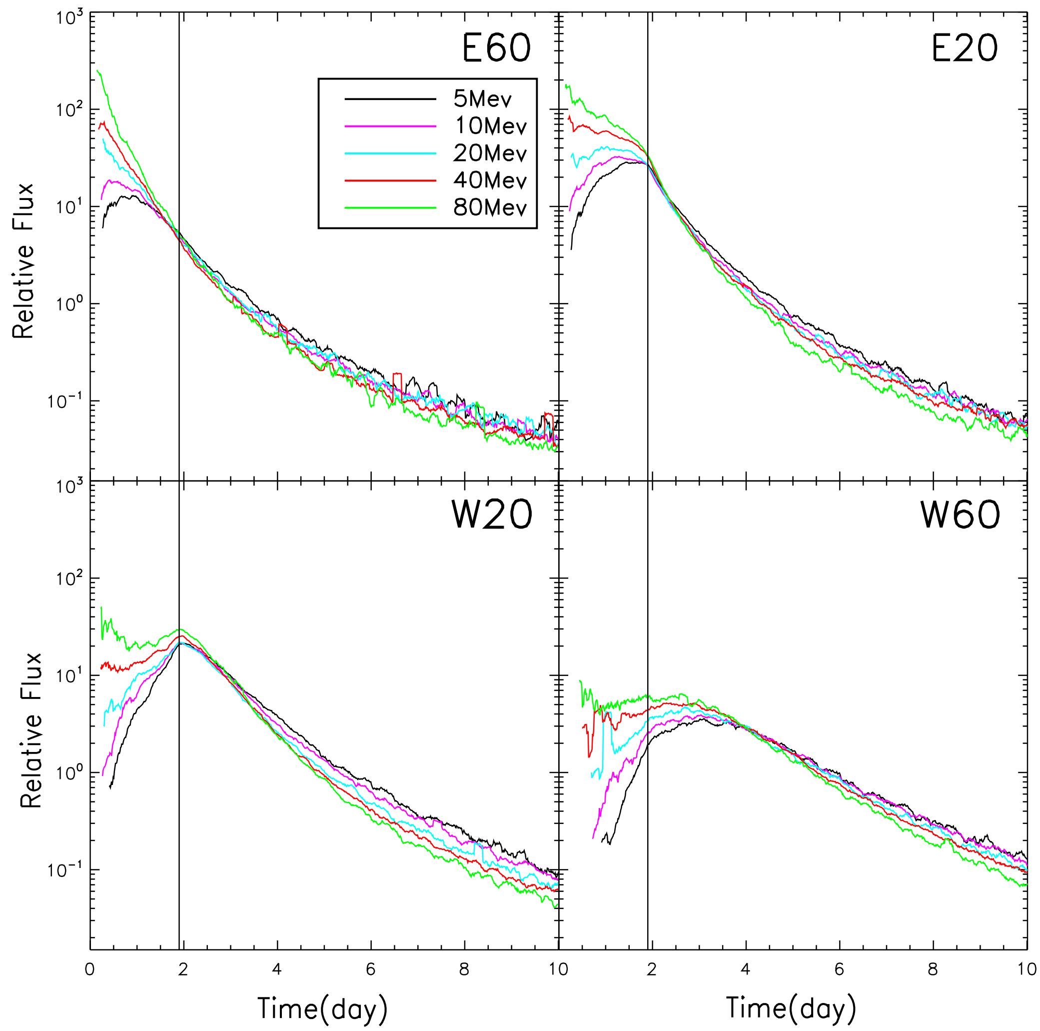

Figure 1. Comparison of different energy protons detected by observers in the 1 AU ecliptic at different longitudes. The fluxes are normalized so their values are similar after all of them reach peaks. The vertical lines indicate the shock's passage of 1 AU. The adiabatic cooling is included in simulations.

energies the fluxes follow a similar trend, then they scatter slowly as time goes by. This is called temporal invariance in the spectra of gradual SEP events. In the E60 event, at all energies the fluxes start to follow a similar trend about one day before the shock passage of 1 AU. In other words, the onset time of the temporal invariance is earlier than the time of the shock passage of the observer. In the E20 and W20 events, however, the onset time of temporal invariance is close to the shock passage of the observers. Furthermore, in the W60 event, the temporal invariance starts the latest; specifically, it starts two days later than the shock arrival.

In Figure 2, the adiabatic cooling is not included in the SEP propagation process. Without adiabatic cooling, shock acceleration strength, and parallel and perpendicular diffusion are the major factors in the decay phase. Due to the different diffusion coefficients and shock acceleration strengths for different energy particles, the fluxes consequently decay with different ratios. With higher energies, the fluxes decay much faster. In these cases, the temporal invariance does not exist in the decay phase.

Comparing Figures 1 and 2, the fluxes decrease much faster with adiabatic cooling. Because of adiabatic energy loss, particles have less energy when they are observed than when they are released in the sources. In addition, since the source spectrum index is negative, the fluxes are lower with higher energies, so the adiabatic cooling effect makes the SEP flux decrease as time passes by. To summarize, the temporal invariance in the spectra results from the adiabatic cooling effect.

3.2. Spatial Invariance in the Spectra

In Figure 3, the SEP fluxes are shown for three observers located at different longitudes, E20, W20, and W60. The upper panel shows the 5 MeV proton fluxes observed. We set two typical time intervals, interval *A*, from 1.3 to 1.5 days in rising phase, and interval *B*, from 6.9 to 7.1 days in the decay phase. In order to study the spatial variance in different phases, in the lower left and right panels of Figure 3, we plot the energy spectra observed in different longitudes in interval *A* and interval *B*, respectively. During interval *A*, the spectra are different among the three observers. However, during interval *B*, spectra are almost the same among the three observers. This phenomenon, which is named spatial invariance in the spectra by Reames et al. (1997), results from the reservoir effect in different energy channels.

Because the shock is a moving source in the interplanetary space, the peak intensity of SEP flux is mainly determined by

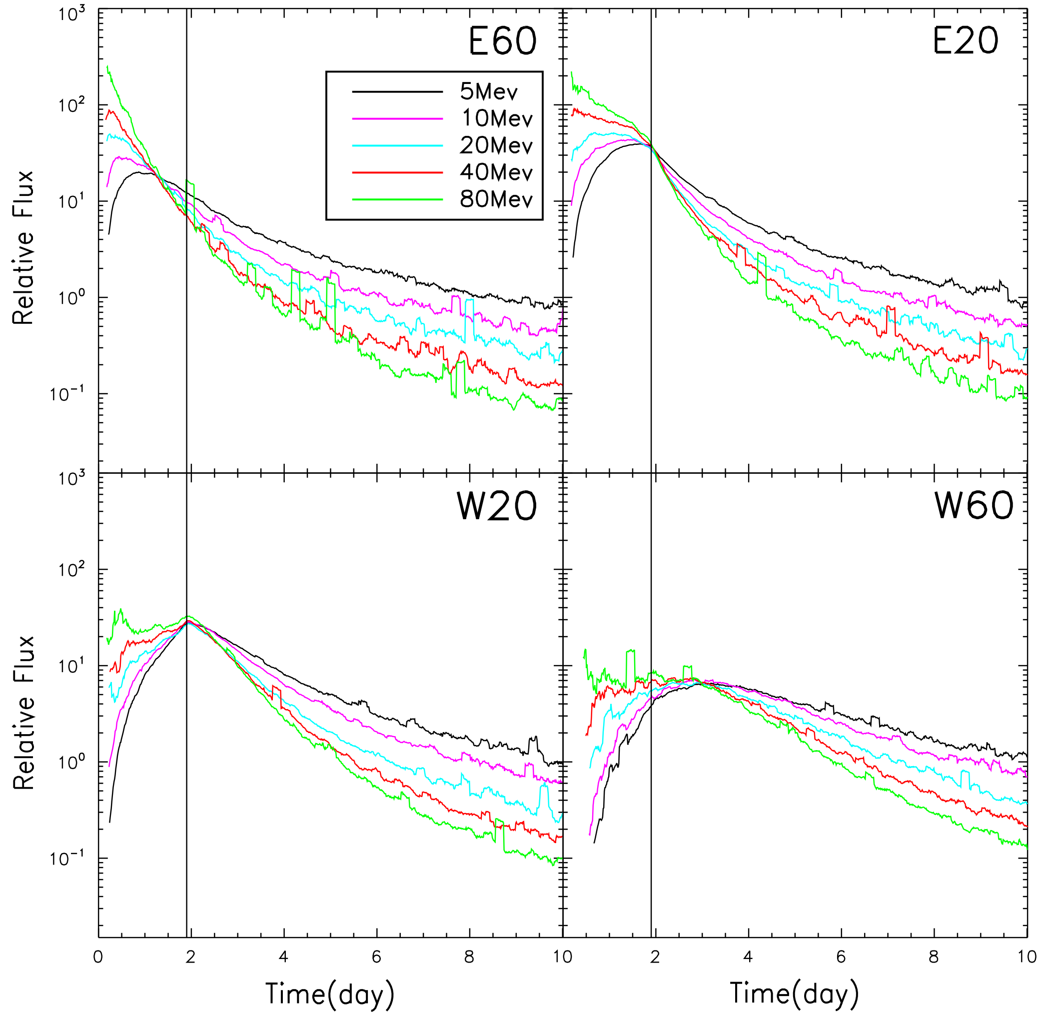

Figure 2. Same as Figure 1 except that the adiabatic cooling is not included.

the shock acceleration strength and parallel MFP. In the upper panel of Figure 3, at the peak time of flux for W20 (W60), the flux for W20 (W60) is close to that for E20. Furthermore, the SEP fluxes decay in a similar ratio because of the effect of adiabatic cooling. At the same time, the latitudinal gradient in the SEP fluxes is further reduced because of the effect of perpendicular diffusion. However, in other simulations with different shock acceleration strengths and parallel MFPs (not shown here), if at the peak time of flux for W20 (W60), the flux for W20 (W60) is significantly different than that for E20, the reservoir phenomenon cannot form in normal diffusion coefficients. As a result, shock acceleration strength, parallel diffusion, and adiabatic cooling are the main factors in forming the reservoir phenomenon, and perpendicular diffusion is a secondary factor.

3.3. Invariant Spectra Region

There are some important characteristics in the invariant spectra region from our simulations (Figure 1). If the observer is located at the eastern flank of the shock, the onset time of invariant spectra is earlier than the shock arrival. But if the observer is located near the central flank of the shock, the spectra invariance begins approximately at the shock passages. Finally, if the observer is located at the western flank of shock, the onset time of invariant spectra is much later than the shock's arrival. From these results, we can better understand the invariant spectra region.

Figure 4 shows the invariant spectra region. In the picture the green line is plotted by Reames et al. (1997), and the red line stems from this work. According to Reames et al. (1997), the left side of the green line is the invariant spectra region, with the assumption that particles are quasi-trapped in the region behind the ICME, and the SEP fluxes gradually decrease as a result of parallel diffusion and adiabatic deceleration mechanisms, in addition to some leakage of energetic particles from ICMEs to the eastern side of the upstream shock. In this sense, ICMEs play a pivotal role in the decay phase of fluxes. As a result, the invariant spectra region is determined by ICMEs' propagation path plus some eastern side of the upstream region. However, we suppose the invariant spectra region could be on the left side of the red line instead. In our simulations, ICME is not included, but in the propagation process perpendicular diffusion is included to reduce the spatial gradient in the fluxes, and adiabatic cooling is included to reduce the temporal variance. As the simulation results showed above, the spatial and temporal of the spectra invariance could result from the effects of shock acceleration strength, adiabatic cooling, and perpendicular diffusion. In this sense, it is possible that the invariant spectra region is not

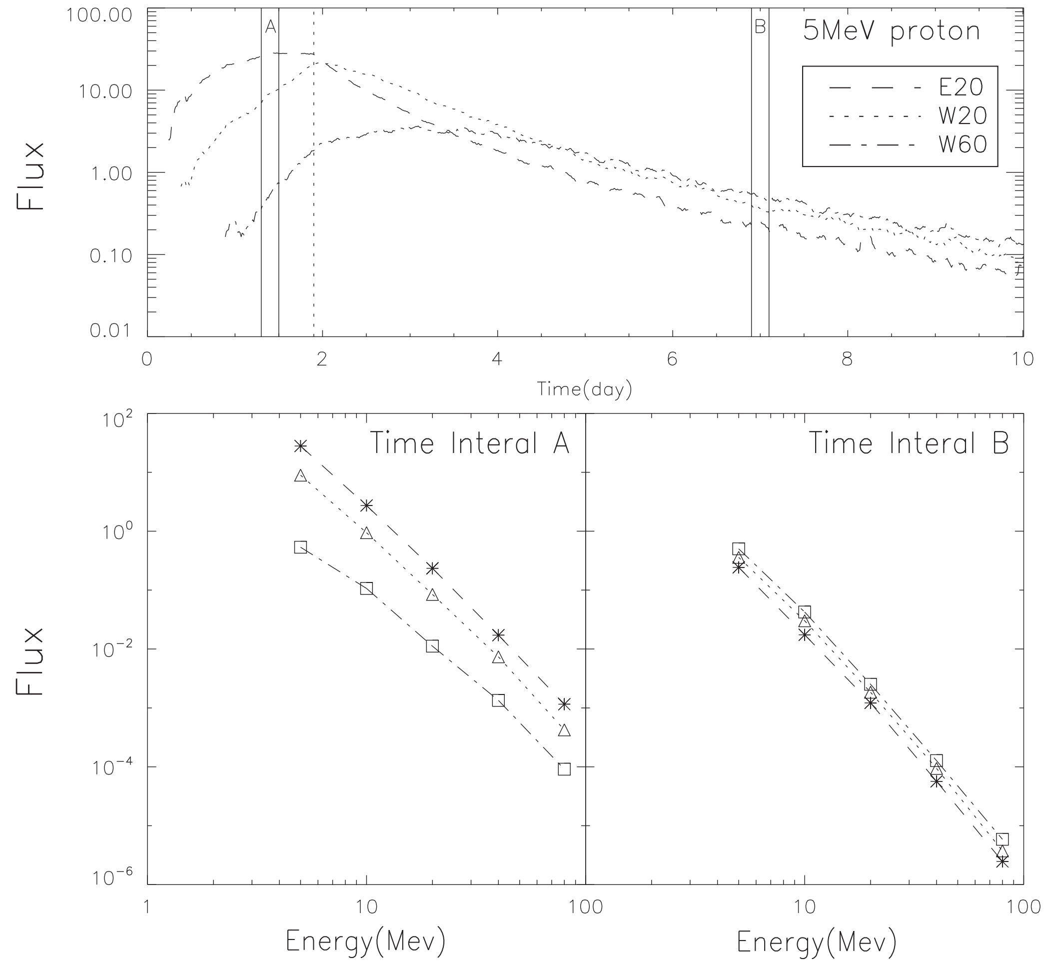

Figure 3. In the upper panel, comparison of 5 MeV protons flux observed in 1 AU ecliptic at different longitudes. The lower left and right panels show the spectra observed at different longitudes during time intervals *A* and *B*, respectively. The vertical dashed lines indicate the shock passage of 1 AU.

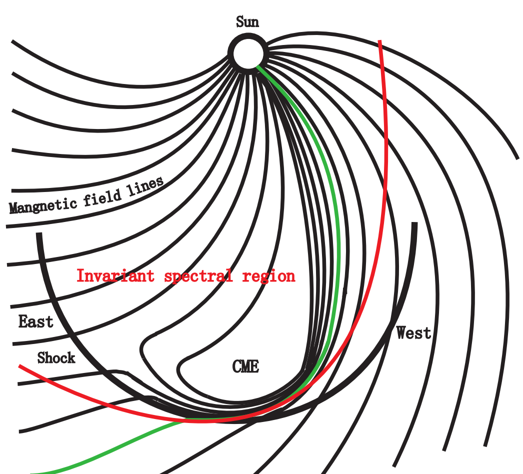

Figure 4. Green line indicates the original spectra invariant region proposed by Reames et al. (1997). The red line indicates a new spectra invariant region based on the simulation results in this paper.

confined by the ICMEs' propagation path. Instead, the invariant spectra region could be confined by the interplanetary shock, but the region expands faster (slower) than the shock at the eastern (western) flank.

4. DISCUSSION AND CONCLUSIONS

We have studied interplanetary shock accelerated SEPs' propagation in three-dimensional IMF. The spectra observed by different observers have been calculated, and the spatial and temporal invariance in the spectra have been reproduced in the simulations. The following are our major findings.

The adiabatic cooling effect is the key factor for forming temporal invariance in the spectra. By including the adiabatic cooling, for different energy channels, the flux decay ratios are almost the same. The temporal invariance results from the fact that all energy particles decay at the same ratio because of the adiabatic cooling effect. At the eastern flank of the shock, the onset time of the spectra invariance is earlier than the shock arrival. For the central cases, however, the onset time of the spectra invariance is close to the time of shock arrival. Finally, at the western flank of the shock, the onset time of the spectra invariance is later than shock arrival. In addition, the fluxes decay much faster in the cases with adiabatic cooling. Without adiabatic cooling, the decay phase of SEP fluxes is dominated by shock acceleration strength, parallel diffusion, and perpendicular diffusion, which all vary with particles' energies. Therefore, the temporal invariance does not exist without adiabatic cooling.

Shock acceleration strength, parallel diffusion, adiabatic cooling, and perpendicular diffusion are four important factors in forming the spatial invariance, which is in reservoir phenomenon in different energy channels. Shock acceleration strength parameters α and ϕ_c are set to 2° and 15° for 5 MeV protons in our simulations, respectively. These parameters also change with the momentum $\alpha \sim p^{0.3}$, $\phi_c \sim p^{-0.3}$, because the shock acceleration strength decreases with higher energy particles. Among the four factors, shock acceleration strength, parallel diffusion, and adiabatic cooling are the main factors in forming the the reservoir phenomenon, and perpendicular diffusion is a secondary factor. This conclusion is derived from our simulations, and it is also consistent with the observations. In Reames et al. (1997) and Reames (2013), a gradual SEP event was detected by *Helios 1*, *Helios 2*, and *IMP 8* during 1979 March 1–March 11. In this event, the reservoir phenomenon appeared, and the onset times of SEPs observed by different spacecraft are very close because of the effect of perpendicular diffusion. At the peak time of flux observed by *Helios 2* (*IMP 8*), the flux observed by *Helios* 2 (*IMP* 8) is close to that observed by *Helios 1*. The importance of the peak intensity of SEP flux observed by *Helios 2* and *IMP 8* in forming the reservoir phenomenon is also noticed by Reames (2013); however, the reservoir phenomenon is explained as a result of the disturbance of the IMF caused by ICMEs. In our model, the peak of the flux is mainly determined by shock acceleration strength and parallel diffusion. Furthermore, the SEP fluxes decay at a similar ratio because of the effect of adiabatic cooling. At the same time, the latitudinal gradient in the SEP fluxes is further reduced because of the effect of perpendicular diffusion. Finally, according to our model, the reservoir phenomenon appeared in this SEP event with the effects of shock acceleration strength, parallel diffusion, adiabatic cooling, and perpendicular diffusion. Observationally, shock acceleration strength, diffusion coefficients, and adiabatic cooling change significantly in different SEP events (Kallenrode 1996, 1997). As a result, the reservoir phenomenon can only form in some gradual SEP events with those controlling effect parameters in appropriate values.

Based on our simulations, we propose a new invariant region. This new region is different from the one proposed by Reames et al. (1997). There are two important characteristics in our new region. First, if the observer is located at the eastern (western) flank of the shock, the onset time of temporal invariant in the spectra is earlier (later) than the shock arrival. Second, the spatial invariance in the spectra can also be formed without ICMEs. These two characteristics are supported by observations, but are difficult to explain using the previous model offered by Reames et al. (1997).

In our model, for simplicity, we ignore the disturbance of the IMF caused by ICME. In principle, the disturbance in the magnetic field can help particles redistribute in space. In future work, we intend to include a realistic three-dimensional ICME shock so that the SEP acceleration and transport in the heliosphere can be investigated more precisely.

The authors thank the anonymous referee for valuable comments. We are partly supported by grants NNSFC 41374177, NNSFC 41125016, and NNSFC 41304135, the CMA grant GYHY201106011, and the Specialized Research Fund for State Key Laboratories of China. The computations were performed by Numerical Forecast Modeling R&D and the VR System of State Key Laboratory of Space Weather and Special HPC work stand of Chinese Meridian Project.

REFERENCES

Beeck, J., & Wibberenz, G. 1986, ApJ, 311, 437
Dresing, N., Gómez-Herrero, R., Klassen, A., et al. 2012, SoPh, 281, 281
Dröge, W., Kartavykh, Y. Y., Klecker, B., & Kovaltsov, G. A. 2010, ApJ, 709, 912
Dwyer, J. R., Mason, G. M., Mazur, J. E., et al. 1997, ApJL, 490, L115
Earl, J. 1974, ApJ, 193, 231
Giacalone, J., Jokipii, J., & Mazur, J. 2000, ApJL, 532, L75
Gordon, B. E., Lee, M. A., Möbius, E., & Trattner, K. J. 1999, JGR, 104, 28263
Guo, F., & Giacalone, J. 2014, ApJ, 780, 16
Hasselmann, K., & Wibberenz, G. 1968, Z. Geophys., 34, 353
He, H.-Q., Qin, G., & Zhang, M. 2011, ApJ, 734, 74
Heras, A. M., Sanahuja, B., Lario, D., et al. 1995, ApJ, 445, 497
Heras, A. M., Sanahuja, B., Smith, Z. K., Detman, T., & Dryer, M. 1992, ApJ, 391, 359
Jokipii, J. R. 1966, ApJ, 146, 480
Kallenrode, M. 1996, JGR, 101, 24393
Kallenrode, M. 1997, JGR, 102, 22347
Kallenrode, M. 2001, JGR, 106, 24989
Kallenrode, M., & Wibberenz, G. 1997, JGR, 102, 22311
Kóta, J., & Jokipii, J. R. 2000, ApJ, 531, 1067
Kóta, J., Manchester, W. B., Jokipii, J. R., de Zeeuw, D. L., & Gombosi, T. I. 2005, in AIP Conf. Ser. 781, The Physics of Collisionless Shocks: 4th Annual IGPP Int. Astrophysics Conf., ed. G. Li, G. P. Zank & C. T. Russell (Melville, NY: AIP), 201
Lario, D., Aran, A., Agueda, N., & Sanahuja, B. 2007, AdSpR, 40, 289
Lario, D., Kallenrode, M.-B., Decker, R. B., et al. 2006, ApJ, 653, 1531
Lario, D., Roelof, E. C., Decker, R. B., & Reisenfeld, D. B. 2003, AdSpR, 32, 579
Lario, D., Sanahuja, B., & Heras, A. M. 1998, ApJ, 509, 415
Lee, M. A. 1983, JGR, 88, 6109
Li, G., Zank, G. P., & Rice, W. K. M. 2003, JGRA, 108, 1082
Li, G., Zank, G. P., & Rice, W. K. M. 2005, JGRA, 110, 6104
Maclennan, C. G., Lanzerotti, L. J., & Hawkins, S. E. 2001, in Proc. 27th ICRC, 8, 3265
Matthaeus, W. H., Qin, G., Bieber, J. W., & Zank, G. P. 2003, ApJL, 590, L53
Mazur, J., Mason, G., Dwyer, J., et al. 2000, ApJL, 532, L79
McKibben, R. B. 1972, JGR, 77, 3957
McKibben, R. B., Connell, J. J., Lopate, C., et al. 2001b, in Proc. 27th ICRC, 8, 3281
McKibben, R. B., Lopate, C., & Zhang, M. 2001a, SSRv, 97, 257
Ng, C. K., Reames, D. V., & Tylka, A. J. 2003, ApJ, 591, 461
Ng, C. K., Reames, D. V., & Tylka, A. J. 2012, in AIP Conf. Ser. 1436, Physics of the Heliosphere: A 10 Year Retrospective, ed. J. Heerikhuisen et al. (Melville, NY: AIP), 212
Potgieter, M. S., & Moraal, H. 1985, ApJ, 294, 425
Qin, G., Matthaeus, W. H., & Bieber, J. W. 2002a, ApJL, 578, L117
Qin, G., Matthaeus, W. H., & Bieber, J. W. 2002b, GeoRL, 29, 1048
Qin, G., & Shalchi, A. 2009, ApJ, 707, 61
Qin, G., & Shalchi, A. 2012, AdSpR, 49, 1643
Qin, G., & Shalchi, A. 2014, PhPl, 21, 042906
Qin, G., Wang, Y., Zhang, M., & Dalla, S. 2013, ApJ, 766, 74
Qin, G., & Zhang, L.-H. 2014, ApJ, 787, 12
Qin, G., Zhang, M., & Dwyer, J. R. 2006, JGRA, 111, 8101
Qin, G., Zhang, M., Dwyer, J., Rassoul, H., & Mason, G. 2005, ApJ, 627, 562
Reames, D. V. 1995, RvGeS, 33, 585
Reames, D. V. 1999, SSRv, 90, 413
Reames, D. V. 2010, SoPh, 265, 187
Reames, D. V. 2013, SSRv, 175, 53
Reames, D. V., Barbier, L. M., & Ng, C. K. 1996, ApJ, 466, 473
Reames, D. V., Kahler, S. W., & Ng, C. K. 1997, ApJ, 491, 414
Rice, W. K. M., Zank, G. P., & Li, G. 2003, JGRA, 108, 1369
Roelof, E. C., Gold, R. E., Simnett, G. M., et al. 1992, GeoRL, 19, 1243
Schlickeiser, R. (ed.) 2002, Cosmic Ray Astrophysics (Berlin: Springer)
Shalchi, A., Bieber, J. W., Matthaeus, W. H., & Qin, G. 2004, ApJ, 616, 617
Shalchi, A., Li, G., & Zank, G. P. 2010, Ap&SS, 325, 99
Skilling, J. 1971, ApJ, 170, 265
Sokolov, I. V., Roussev, I. I., Gombosi, T. I., et al. 2004, ApJL, 616, L171
Tan, L. C., Reames, D. V., Ng, C. K., Saloniemi, O., & Wang, L. 2009, ApJ, 701, 1753
Tylka, A. J., & Lee, M. A. 2006, ApJ, 646, 1319
Verkhoglyadova, O. P., Li, G., Zank, G. P., Hu, Q., & Mewaldt, R. A. 2009, ApJ, 693, 894
Verkhoglyadova, O. P., Li, G., Zank, G. P., et al. 2010, JGRA, 115, 12103
Wang, Y., Qin, G., & Zhang, M. 2012, ApJ, 752, 37

Wang, Y., Qin, G., Zhang, M., & Dalla, S. 2014, ApJ, 789, 157
Zank, G. P., Rice, W. K. M., & Wu, C. C. 2000, JGR, 105, 25079
Zhang, M. 1999, ApJ, 513, 409
Zhang, M., Jokipii, J. R., & McKibben, R. B. 2003, ApJ, 595, 493
Zhang, M., Qin, G., & Rassoul, H. 2009, ApJ, 692, 109
Zuo, P., Zhang, M., Gamayunov, K., Rassoul, H., & Luo, X. 2011, ApJ, 738, 168
Zuo, P., Zhang, M., & Rassoul, H. K. 2013, ApJ, 767, 6